Journal of Catalysis **184,** 349–356 (1999)
Article ID jcat.1999.2468, available online at http://www.idealibrary.com on IDEAL®

Dehydrogenation of *i*-Butane on CrO_x/SiO_2 Catalysts

A. Hakuli,* M. E. Harlin,† L. B. Backman,† and A. O. I. Krause†

*Neste Ltd., Corporate Technology, P.O. Box 20, FIN-02151 Espoo, Finland; and †Helsinki University of Technology, Department of Chemical Technology, P.O. Box 6100, FIN-02015 HUT, Finland

Received September 30, 1998; revised February 25, 1999; accepted March 10, 1999

CrO_x/SiO_2 catalysts were characterized and their activity in the dehydrogenation of *i*-butane was measured. Cr loading of the catalysts was between 1.1 and 11 wt% and preparation was by impregnation. The consumption of isolated OH groups of SiO_2 upon deposition of CrO_x was followed by DRIFT-IR. The presence of unreacted OH groups in the calcined catalyst at high loadings of Cr and the formation of α-Cr_2O_3 (XRD) showed, however, the tendency of CrO_x to form clusters rather than a well-dispersed phase on SiO_2. After calcination, 0.8–1.0 wt% Cr was stabilized in 6+ oxidation state (UV-VIS). On the basis of H_2-TPR measurements it was suggested that these Cr^{6+} were stabilized by anchoring on SiO_2 or on the α-Cr_2O_3/SiO_2 formed with increasing Cr loading. The activities of the CrO_x/SiO_2 catalysts were studied in the dehydrogenation of *i*-butane at 540°C by monitoring the product distributions with a rapid FT-IR gas analyzer. The dehydrogenation activity is attributed to redox Cr in 3+ and 2+ oxidation states and tentatively to part of the nonredox Cr^{3+}. The relatively low selectivity of CrO_x/SiO_2 at low loadings of Cr was evidently due to the presence of Cr^{2+} directly anchored to SiO_2.

Key Words: **CrO_x; SiO_2; dehydrogenation of alkanes; FT-IR gas analyzer.**

INTRODUCTION

The activity of CrO_x/Al_2O_3 in the dehydrogenation of alkanes has been studied for decades without complete understanding of the system even now (1). Because of thermodynamic requirements, dehydrogenation is typically performed at relatively high temperatures. The high temperature, together with the presence of hydrocarbons and hydrogen in the gas phase, generates conditions where calcined CrO_x/Al_2O_3 is reduced (2–11). Cr^{6+} or Cr^{5+} in the calcined catalysts is therefore proposed to be inactive in dehydrogenation and the dehydrogenation activity to be due to redox Cr^{3+} formed from Cr^{6+} or Cr^{5+} (2, 4–9, 11). More precisely, DeRossi *et al.* (4) propose that the active sites are mononuclear Cr^{3+} with two coordinative vacancies. Study of CrO_x/Al_2O_3 with a wide range of Cr loadings has indicated, nevertheless, that the dehydrogenation activity cannot be explained by the redox Cr^{3+} species alone (8, 9, 11) because the activity increases continuously with Cr loading, whereas the concentration of redox Cr^{3+} levels off. The amount of nonredox Cr^{3+} sites increases drastically with Cr loading, however, and their role as additional active sites was proposed (9, 11). The negligible activity of nonredox Cr^{3+} at low Cr loadings was attributed to their stabilization in or on Al_2O_3 lattice rendering them catalytically inactive (11). The strong interaction between Cr^{3+} and Al_2O_3 can be understood in terms of the closeness of the ionic radii and charge of Cr^{3+} and Al^{3+}. Cr^{3+} can thus relatively easily diffuse into vacant octahedral Al^{3+} sites (12).

In addition to the evident dehydrogenation activity of redox and nonredox Cr^{3+}, some earlier papers (13–16) and the recent paper by Slovetskaya *et al.* (17) suggest that Cr^{2+} on Al_2O_3 or SiO_2 is active as well. Ashwamy *et al.* (14) have suggested that the activity of Cr^{2+} is even higher than that of Cr^{3+}. With these findings in view, the aim of the present work was to study the dehydrogenation activity of Cr^{2+} by characterizing and measuring the activity of a series of CrO_x/SiO_2 catalysts with a wide range of Cr loadings. The SiO_2 support was selected because, when supported on SiO_2, Cr is relatively easily reduced to 2+ oxidation state (1, 18–20). Formation of Cr^{2+} on Al_2O_3 is more difficult owing to the stabilizing effect exerted by the structure of Al_2O_3 on Cr^{3+} (1, 21).

METHODS

Preparation of CrO_x/SiO_2

The catalyst support was GRACE Davison SiO_2 (S 432) with a particle size of 0.25–0.50 mm and surface area of 317 m^2/g determined after calcination at 580°C for 18 h. The number of OH groups on the corresponding SiO_2 was 1.9 OH/nm^2 of which 1.5 and 0.4 OH/nm^2 were determined by NMR to be isolated and H bonded, respectively (22). Prior to impregnation, the SiO_2 support was dried at 200°C for 2 h under vacuum. CrO_x/SiO_2 catalysts were prepared by incipient wetness impregnation technique from aqueous solution of $Cr(NO_3)_3 * 9H_2O$ (>97%, Fluka). The samples were stored overnight at room temperature, dried at 60°C for 16 h under vacuum, and calcined in synthetic air at 570°C for 13 h. Notations such as CrS(1.1) are employed

0021-9517/99 $30.00

for the catalysts with the value in parenthesis indicating the Cr loading. The reference sample of bulk α-Cr_2O_3 (99%, Riedel-deHaën) was used after calcination at 570°C for 5 h ($\approx$5 m^2/g).

Characterization of CrO_x/SiO_2

Cr concentration of the catalyst samples was measured by instrumental neutron activation analysis (INAA) (23). Cr^{6+} in the samples was determined by UV-VIS spectrophotometry (23). After the sample was heated in a muffle furnace for 1 h at 560°C, Cr^{6+} was dissolved as CrO_4^{2-} from the samples with deionized water or NaOH. The amount of extracted CrO_4^{2-} did not differ with the dissolving agent (water or NaOH). In this method, Cr^{5+}, if present in the sample, may be dissolved together with Cr^{6+} (6). The amount of Cr^{5+} in the supported catalysts was assumed to be very small, however (1, 6, 21, 24), not exceeding a few percent of the total amount of Cr (6, 21). Furthermore, Cr^{6+} was assumed to be the main species formed in the calcination of bulk α-Cr_2O_3 (25–28).

Surface areas of the catalysts were determined with a Coulter Omnisorp 100CX (static volumetric method). The distribution of Cr in the support was studied by scanning electron microscopy (SEM) and energy dispersive X-ray spectroscopy (EDS). The measurements were carried out with a JEOL JSM-840A scanning electron microscope equipped with a PGT Omega Light Element SiLi detector and fitted with IMIX version 6.860 software. Before the measurement the catalyst particles were embedded in epoxy resin, and cross-sections of particles were cut with a glass-knife microtome. The samples were coated with carbon to prevent charging under the electron beam. The crystalline structure of the catalysts was studied by X-ray diffraction analysis (XRD) with a Phillips PW diffractometer MDP 1880 using Cu$K\alpha$ radiation. A Nicolet Impact 400D FT-IR spectrometer was used for the diffuse reflectance spectroscopy measurements. The measurements were performed in an accessory kept in a glove-box under nitrogen atmosphere. The spectra were measured from grounded samples at 2 cm^{-1} resolution with a signal averaging 50 scans. The spectra were compared after background subtraction and normalizing according to SiO_2 lattice vibration at 1865 cm^{-1}.

Temperature programmed reduction (H_2-TPR) measurements were performed with an Altamira Instruments AMI-100 catalyst characterization system. The catalyst samples (50 mg) were flushed with helium at 150°C for 30 min and cooled down to 30°C. After that the samples were heated from 30 to 560°C at a rate of 10°C/min under a flow of 5 vol% O_2/He mixture. The sample was kept at 560°C for 30 min and then cooled down to 30°C under flowing O_2/He (29). The sample was flushed with argon where after the TPR was performed at a heating rate of 5°C/min to 560°C under a flow of 10 vol% H_2/Ar mixture (30 cm^3/min). The consumption of hydrogen was monitored by a thermal conductivity detector (TCD). The relative amounts of H_2 consumed at different temperature intervals were estimated by fitting Gaussian peaks to the TPR profiles. Successful modeling of the profiles sometimes required more than one Gaussian peak.

Dehydrogenation Activity

The activities of the catalysts were measured in the dehydrogenation of *i*-butane at 540°C under atmospheric pressure. The reactor consisted of an automated laboratory-scale flow reactor and an on-line FT-IR gas analyzer with program for the analysis of IR spectra (Gasmet, Temet Instruments Ltd.) (7, 8, 30). The catalyst (200 mg) was heated to the reaction temperature under 5% O_2/N_2 flow (O_2 99.5%, N_2 99.999%, AGA) and was flushed there for 3 h. The activity of the calcined catalyst was tested in three consecutive dehydrogenation cycles, in between which the catalyst was regenerated with diluted air. The dehydrogenation feed consisted of 10 vol% *i*-butane (99.95% AGA) in nitrogen (99.999%, AGA) with a gas flow of 66 cm^3/min (STP). The nitrogen used was further purified with an Oxisorb (Messer Griesheim). The dehydrogenation and oxidation periods were 10 and 30–50 min, respectively. In between, the catalyst was purged with nitrogen for 30 min. Two of the catalysts (i.e., CrS(1.1) and CrS(11)) were also tested by reducing the catalyst at 540°C for 30 min with 5 vol% H_2/N_2 mixture (99.999%, AGA) before the start of the *i*-butane feed. At 540°C and the partial pressure of 10.1 kPa *i*-butane in the feed, the thermodynamic equilibrium conversion for the dehydrogenation of *i*-butane to *i*-butene is 80%.

The product mixture was monitored with a FT-IR gas analyzer (850–4000 cm^{-1} with a resolution of 8 cm^{-1} at a scanning rate of 10 scans/s) (7, 8, 30) The cuvette (9 cm^3) was maintained at constant temperature (175°C) and pressure (103 kPa). The sample spectra were interpreted with reference to a set of calibration spectra of pure compounds diluted in nitrogen (methane, ethane, ethene, propane, propene, *i*-butane, *i*-butene, *n*-butane, 1-butene, *cis*-2-butene, trans-2-butene, 1,3-butadiene, CO, CO_2, benzene, toluene, and water). The residuals in the fitting of the sample spectra with the set of calibration spectra were less than 3% of the sample spectra . The conversions and selectivities were calculated from the reaction products, either by neglecting the amount of coke deposited in the catalyst or by including the coke in the calculations. The amount of coke deposited was obtained from the amounts of CO and CO_2 evolved during the regeneration of the catalysts *in situ* at 540°C. In the calculation of the selectivity to butenes all four isomers were included (*i*-, 1-, *cis*-2-, and *trans*-2-butene). The mass balance for C was better than 99%.

TABLE 1

Cr Contents, BET Surface Areas, Cr^{6+} Concentrations, and Formation of α-Cr_2O_3 in CrO_x/SiO_2 Catalysts Calcined at 570°C

Sample	Cr wt%	Cr at/nm^2	BET m^2/g	Cr^{6+} wt%	α-Cr_2O_3 (XRD)
CrS(1.1)	1.1	0.41	309	0.79	–
CrS(3.4)	3.4	1.3	308	0.99	+
CrS(8.7)	8.7	3.3	308	1.03	+
CrS(11)	11	4.5	283	0.79	+

RESULTS

Characterization of CrO_x/SiO_2

Physico-chemical properties. CrO_x/SiO_2 catalysts were prepared by incipient wetness impregnation technique with 1.1, 3.4, 8.7, and 11 wt% Cr (Table 1). SEM-EDS measurements indicated that Cr was evenly distributed through the SiO_2 particles. The specific surface area of the catalysts was unchanged relative to that of the support except for an 11% smaller area for CrS(11). The XRD measurements indicated the presence of crystalline α-Cr_2O_3 in CrS(3.4), CrS(8.7), and CrS(11).

Binding of CrO_x on SiO_2. The binding of CrO_x to SiO_2 was studied by comparing the DRIFT-IR spectra of the calcined catalysts with the spectrum of the support. Upon deposition of CrO_x, the band of isolated OH groups of SiO_2 at 3745 cm^{-1} (31–32) decreased in intensity. However, not all the isolated OH groups (1.5 OH/nm^2) were reacted even in CrS(11) (4.5 Cr/nm^2). In addition to the 3745 cm^{-1} band the spectra of the calcined catalysts exhibited small and broad bands in the region of H-bonded OH groups.

Oxidation state distribution after calcination. After calcination, the amount of Cr^{3+} in CrS(1.1) oxidized to Cr^{6+} was 0.8 wt% Cr (0.3 at/nm^2), this being 72% of the total amount of Cr (Table 1). The amounts of Cr^{6+} in CrS(3.4) and CrS(8.7) were slightly higher, being 1.0 wt%, but the amount in CrS(11) was lower again. It is noteworthy that in CrS(11) only 7% of Cr^{3+} was oxidized. On bulk α-Cr_2O_3, the amount of Cr^{6+} was 0.08 wt% (1.6 at/nm^2). If it is assumed that the number of surface Cr atoms in bulk α-Cr_2O_3 is 11 Cr/nm^2 (16), then 15% of the surface Cr were oxidized to Cr^{6+}.

Reduction of CrO_x/SiO_2 (H_2-TPR). The H_2 consumptions of the calcined catalysts and of bulk α-Cr_2O_3 as a function of temperature are shown in Fig. 1. The H_2 consumption of CrS(1.1) exhibited a single maximum at 430°C. With increasing Cr content, a second maximum appeared at 270°C, with a shoulder at 305°C. The relative intensity of the low temperature maximum at 255–270°C and that of the shoulder at 300–305°C increased with Cr loading, while the maximum at 420–430°C decreased. The low temperature maxima observed for the supported catalysts coincided well with the maximum observed for bulk α-Cr_2O_3 at 260°C with a shoulder at 295°C.

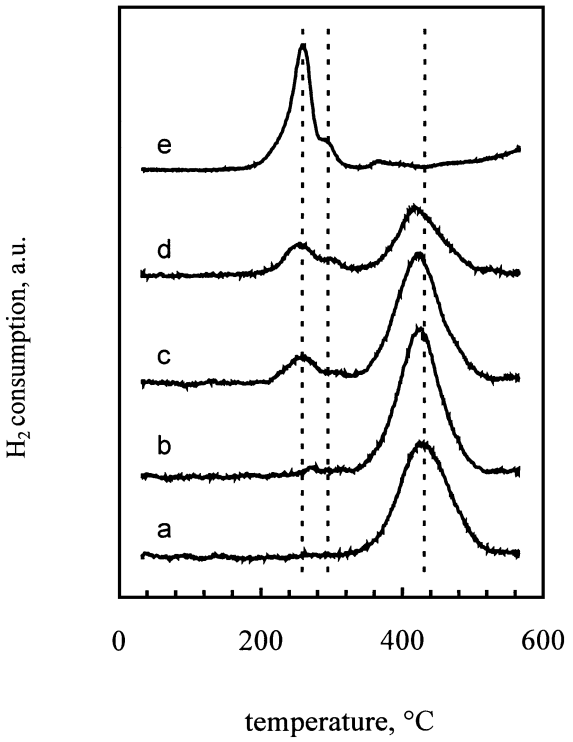

FIG. 1. H_2 consumption of (a) CrS(1.1), (b) CrS(3.4), (c) CrS(8.7), (d) CrS(11), and (e) bulk α-Cr_2O_3.

The extent of the reduction of Cr^{6+} in the catalysts was calculated from the H_2 consumption by assuming that (i) H_2 was consumed only in the reduction of Cr^{6+} species, (ii) reduction yielded Cr^{3+} and Cr^{2+} species, and (iii) hydrogen consumption was 2 and 1.5 mol H_2/mol Cr^{6+} for the formation of Cr^{2+} and Cr^{3+}, respectively. The H_2 consumption of CrS(1.1) corresponded to reduction of Cr^{6+} to 2+ oxidation state (Table 2). With increasing Cr loading, H_2 consumption relative to the amount of Cr^{6+} decreased, indicating formation of Cr^{3+} together with Cr^{2+}.

TABLE 2

H_2 Consumption of the Calcined Catalysts, and the Concentrations of Cr^{2+} and Cr^{3+} Formed in the Reduction of Cr^{6+}

Sample	H_2 consumption mol H_2/mol Cr^{6+}	Cr^{2+} wt%	Cr^{3+} wt%
CrS(1.1)	2.03	0.79	0
CrS(3.4)	1.86	0.71	0.28
CrS(8.7)	1.79	0.60	0.43
CrS(11)	1.59	0.13	0.66
α-Cr_2O_3	2.14	0.08	0

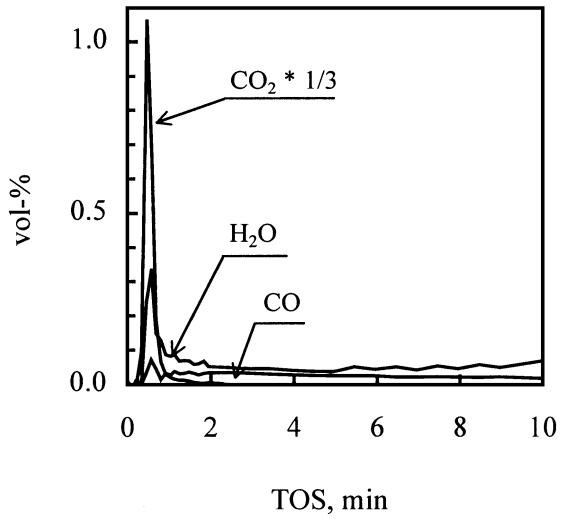

FIG. 2. Reduction of calcined CrS(11) under dehydrogenation conditions (10 vol% *i*-butane) at 540°C.

Dehydrogenation Activity

Calcined CrO_x/SiO_2. The activities of CrO_x/SiO_2 during 10 min on stream were studied in the dehydrogenation of *i*-butane at 540°C. During the first minute on stream, Cr^{6+} was reduced by *i*-butane detected as an instant release of CO_2, CO, and H_2O (Fig. 2). CO and H_2O were evolved in low concentrations until the reaction was halted. It is noteworthy that the amount of released H_2O was less than that calculated from the amounts of released CO_2 and CO, and by assuming a reduction of Cr^{6+} by *i*-butane. At 1 min on stream, the ratios of oxygen abstracted from Cr^{6+} in reduction (as calculated from the amount of evolved CO_2, CO, and stoichiometric amount of water) to the original amount of Cr^{6+} were 1.52–1.85 mol/mol, depending on the Cr loading. With longer time on stream, the ratios increased to 1.55–2.00 mol/mol, approaching the values obtained for the reduction by H_2-TPR (see Table 2).

The average activity of the catalysts between 1 and 10 min on stream increased with the Cr loading, but the detailed behavior varied with the loading (Fig. 3): The activity of CrS(1.1) decreased over the 10 min, whereas the activities of CrS(8.7) and CrS(11) increased between 1 and 3 min and then declined. On CrS(3.7) the activity remained constant between 1 and 2 min and declined with longer time on stream. The behavior of the catalysts in three consecutive 10-min reaction cycles, with regeneration with diluted oxygen in between, was repeatable except for a slight decrease in activity with the number of cycles.

In addition to *i*-butene, products attributed to molecular cracking such as propane, propene, and methane were detected in the product flow. Isomers of *i*-butene (1-, *cis*-2-, and *trans*-2-butene) and 1,3-butadiene were observed in very small concentrations. The selectivities to butenes were constant during the 10-min reaction cycle (not shown in Fig. 3) and they increased slightly with the Cr loading from 78 to 84%. The improvement in the selectivities of the catalysts with Cr loading was confirmed by a formation of less methane (−33%) and propene (−43%) on CrS(8.7) than on CrS(3.6) when the selectivities of the catalysts were compared at the same conversion level (by changing WHSV).

The conversions, selectivities, and yields that include the coke formation were calculated from the amounts of carbon oxides evolved during the *in situ* regeneration of the catalyst and by averaging the concentrations of each gaseous reaction product formed during the 10 min on stream (Table 3). With increasing Cr loading, the cracking and coke formation decreased, whereas selectivity to butenes and the overall conversion increased.

The activity and selectivity of bulk α-Cr_2O_3 was measured for comparison. Similar to the supported samples the reduction of Cr^{6+} by *i*-butane was seen as a release of CO_2, CO, and H_2O immediately after exposure of the catalyst to the feed. The activity of bulk α-Cr_2O_3 resembled that of CrS(11) and CrS(8.7): the conversion first increased with time on stream and then declined (Fig. 4). Except for the formation of a small amount of *n*-butane the products were the same as observed for the supported samples. The selectivity of bulk α-Cr_2O_3 to butenes was 93% being thus considerably higher than the selectivities of 61–72% measured for the supported catalysts at only slightly higher conversion levels.

H_2-prereduced CrO_x/SiO_2. To understand better the behavior of the catalysts during the first minutes on stream, the activities of Cr(1.1) and Cr(11) were measured after H_2

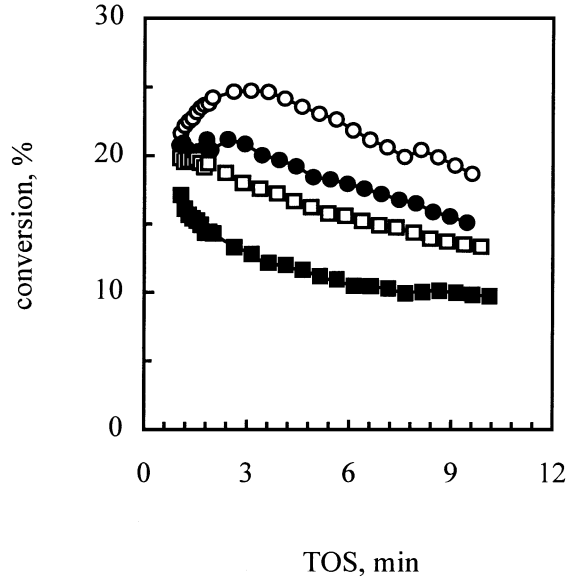

FIG. 3. Activity of calcined CrS(1.1) (■), CrS(3.4) (❑), CrS(8.7) (●), and CrS(11) (❍) in the dehydrogenation of *i*-butane at 540°C

TABLE 3

Conversions, Selectivities, and Yields[a] Including the Amounts of Coke[b] Formed on Calcined and H_2-Prereduced Catalysts in *i*-Butane Dehydrogenation at 540°C

Sample	Conversion of *i*-C_4 %	Selectivity, %					Yield of $C_4^=$ %
		$C_4^=$	$C_4^{==}$	*n*–C_4	C_1–C_3	coke	
CrS(1.1)	16	61	0	0	16	23	10
CrS(3.4)	19	67	1	0	17	15	13
CrS(8.7)	22	67	0	0	13	20	15
CrS(11)	25	72	0	0	13	15	18
α-Cr_2O_3	10	93	0	3	3	1	9
CrS(1.1)–H_2-prereduced	18	54	0	0	8	38	10
CrS(11)–H_2-prereduced	36	68	0	0	8	24	24
α-Cr_2O_3–H_2-prereduced	10	88	0	4	2	6	9

[a] Average of the measured values between 1 and 10 min on stream.
[b] Obtained from the amounts of CO_2 and CO evolved during the regeneration of the samples *in situ* at 540°C.

reduction. The purpose of the prereduction was to separate the reduction of the calcined catalysts from the dehydrogenation. Accordingly, no CO_2 or H_2O was detected, but CO was observed in very small concentration, corresponding to the concentration of CO formed with the calcined catalyst between 1 and 10 min on stream. Since no H_2O was detected in the product flow of the H_2 prereduced catalyst, the formation of a small concentration of CO was not associated with a further reduction of the H_2-prereduced catalyst under dehydrogenation conditions. Instead, CO was probably formed in steam reforming of the hydrocarbons. The source of H_2O for the reforming could have been the H_2O entrapped in the catalyst during the reduction.

The activity of H_2-prereduced CrS(1.1) was constant between 1 and 10 min on stream, and at the same level as the activity of the corresponding catalyst without prereduction after 5 min on stream (Fig. 5). On the other hand, no activation period was observed for H_2-prereduced CrS(11), but the activity was as high as 35% at 1 min on stream and then declined. The effect of H_2 prereduction on the initial activity of bulk α-Cr_2O_3 was similar to the effect on CrS(11): the activity was at maximum at 1 min on stream (Fig. 4). The amount of coke deposited was higher on the H_2-prereduced catalyst than on calcined catalyst, and the selectivities were thus lower (Table 3).

DISCUSSION

Characterization of CrO_x/SiO_2 Catalyst

Binding of CrO_x on SiO_2. With deposition of CrO_x, the band of isolated OH groups of SiO_2 in the spectra of

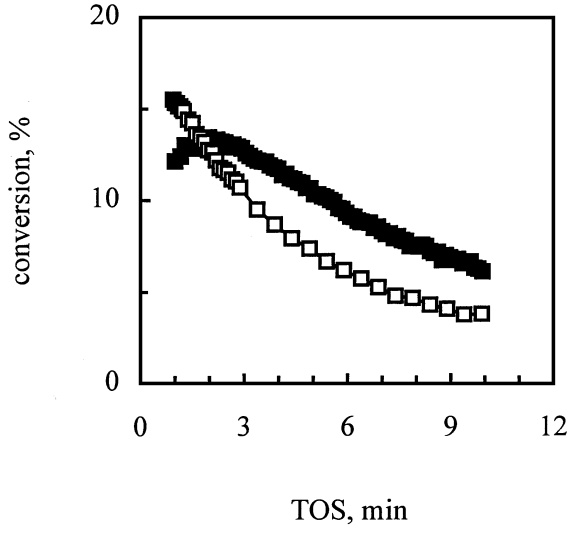

FIG. 4. Activity of calcined (■) and H_2 prereduced (❑) bulk α-Cr_2O_3 in the dehydrogenation of *i*-butane at 540°C.

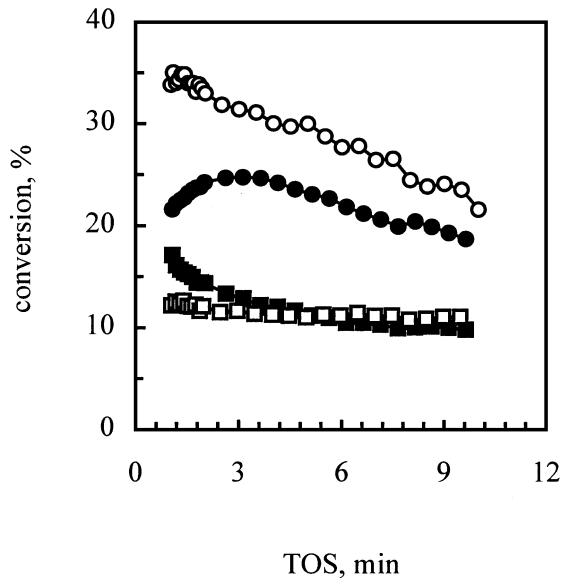

FIG. 5. Activity of H_2 prereduced (open symbols) and calcined (solid symbols) CrS(1.1) (■, ❑) and CrS(11) (●, ❍) in the dehydrogenation of *i*-butane at 540°C.

calcined catalysts decreased in intensity, indicating the consumption of OH groups in the binding of CrO_x. The presence of α-Cr_2O_3 in the calcined catalysts even in CrS(3.4) (1.3 Cr/nm^2), together with unreacted OH groups, illustrates the well-known tendency of CrO_x to form clusters rather than a well-dispersed phase on SiO_2 (6, 12, 19, 28, 33–35).

Cr^{6+} and Cr^{3+} on calcined catalyst. Because bulk CrO_3 is unstable at the calcination temperatures we employed (28, 36, 37), the presence of Cr^{6+} in the supported samples and in bulk α-Cr_2O_3 was attributed to surface oxidation. The Cr^{6+} concentration of the catalysts passed through a maximum with increasing Cr loading: the highest concentration of Cr^{6+} (1.0 wt% or 0.4 Cr/nm^2) was observed in CrS(3.6) and CrS(8.7) (see Table 2). We note that, in our catalysts calcined at 570°C, the Cr^{3+} species existed together with Cr^{6+} even at the loading of 0.4 Cr/nm^2 (1.1 wt% Cr), and their concentration increased dramatically with Cr loading. McDaniel *et al.* (38), on the other hand, have shown that all chromium is oxidized to Cr^{6+} in 650°C samples containing up to 1.1 Cr/nm^2. An explanation for the presence of Cr^{3+} in CrS(1.1) could be that, under our experimental conditions, not all CrO_x was anchored to SiO_2 even at a loading of 0.4 Cr/nm^2, but formed either isolated or clustered structures (12, 35, 39–41).

Environment of Cr^{6+}. Direct interaction between Cr^{6+} and SiO_2 presumably dominates in CrS(1.1) because of the small amount of nonredox Cr^{3+} and the absence of α-Cr_2O_3, (XRD). Comparison of the H_2 consumptions of CrS(1.1) and bulk α-Cr_2O_3, with maxima at 430 and 260°C, respectively, indicated that Cr^{6+}/SiO_2 was more difficult to reduce than Cr^{6+}/α-Cr_2O_3 (see Figs. 1a and 1e) (42). Accordingly, the maxima at 430–420°C and 270–250°C in the H_2 consumptions of CrS(3.4), CrS(8.7), and CrS(11) were interpreted as the presence of both Cr^{6+}/SiO_2 and $Cr^{6+}/Cr_2O_3/SiO_2$ in the catalysts.

Cr^{3+} and Cr^{2+} on reduced surface. The H_2 consumption of bulk α-Cr_2O_3 between 25 and 350°C corresponded to a reduction of Cr^{6+} to 2+ oxidation state. The formation of Cr^{2+} on bulk α-Cr_2O_3 has also been proposed elsewhere (38, 43–45), although Cr^{3+} is considered to be the preferred species. We attributed the presence of two maxima in the H_2 consumption to a stepwise reduction of Cr^{6+} to Cr^{2+} via 3+ oxidation state (see Fig. 1e). The size of the shoulder at 295°C was estimated to be 11% of the size of the main peak, a considerably lower value than the 33% calculated from the stoichiometry of the stepwise reduction. The discrepancy might be due to the uncertainty in the fitting of a main peak and shoulder of nonideal shapes. In CrS(8.7) and CrS(11), the estimated sizes of the shoulders at 300–305°C were 16 and 33% of the main peaks at 255–270°C, respectively. Quantitative calculation of the peaks for CrS(3.4) was not reasonable owing to the weakness of the peaks.

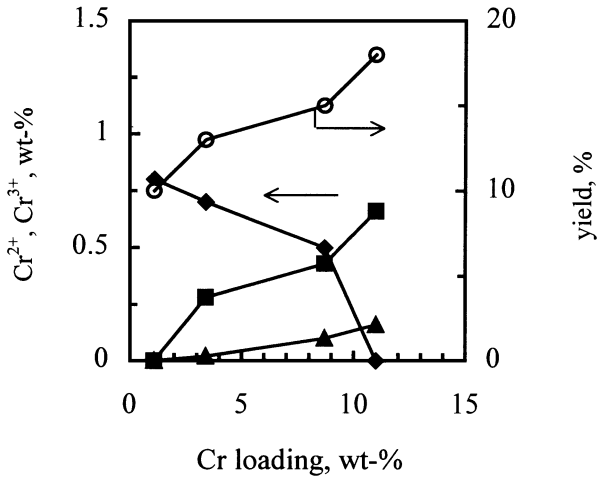

FIG. 6. Dehydrogenation activity (○) and the amounts of redox Cr^{2+}/SiO_2 (◆), Cr^{3+}/SiO_2 (■), and $Cr^{2+}/Cr_2O_3/SiO_2$ (▲) in CrO_x/SiO_2 at different Cr loadings (H_2-TPR).

On the other hand, only one maximum was resolved in the reduction of Cr^{6+}/SiO_2. The extent of the reduction of Cr^{6+}/SiO_2 in CrS(1.1), CrS(3.4), CrS(8.7), and CrS(11) was calculated by subtracting the amount of H_2 consumed in reduction of $Cr^{6+}/Cr_2O_3/SiO_2$ from the total H_2 consumption (Fig. 1). Even though this procedure was not strictly valid since $Cr^{3+}/Cr_2O_3/SiO_2$ may have been formed together with $Cr^{2+}/Cr_2O_3/SiO_2$, the error in the calculation would not change the observed trend (Fig. 6). Namely, with increased Cr loading, the degree of the reduction of Cr^{6+}/SiO_2 decreased, i.e., Cr^{3+}/SiO_2 was formed in addition to Cr^{2+}/SiO_2. It has been proposed by Zecchina *et al.* (46) that the Cr^{6+} monomers present at low loadings of Cr are predominantly reduced to Cr^{2+}, whereas the Cr^{6+} dimers and polymers present at higher Cr loadings are mostly reduced to Cr^{3+}.

Dehydrogenation Activity of CrO_x/SiO_2

Potential active sites. Cr^{6+} was unstable under the reaction conditions for dehydrogenation because it was reduced by the feed or the reaction products. Its activity in dehydrogenation was therefore ruled out, and instead the sites formed in the reduction were of interest, i.e., Cr^{2+}/SiO_2, Cr^{3+}/SiO_2, and $Cr^{2+}/Cr_2O_3/SiO_2$ (or $Cr^{3+}/Cr_2O_3/SiO_2$). In addition, the reduced catalysts contained nonredox Cr^{3+}, the amount of which increased dramatically with Cr loading (XRD and UV-VIS) (see Table 1). On the whole, the extent of the reduction of Cr^{6+} measured by a FT-IR gas analyzer under dehydrogenation conditions was fairly close to the values obtained by H_2-TPR. From this we concluded that the H_2-TPR could suitably be applied to characterize the reduced sites formed under the dehydrogenation conditions.

In the discussion of the active site(s) below, we treat first the observed increase or decrease in the activity of the

calcined catalysts between 1 and 3 min on stream. One possible explanation for the transient behavior could be a progressive desorption or rearrangement of the H_2O (or -OH/-H) entrapped in the catalyst during the reduction. The release of CO_2 and CO in the reduction of the calcined catalyst was not, namely, accompanied by the desorption of a stoichiometric amount of H_2O (see Fig. 2). Entrapped H_2O (or -OH/-H) could have diverse effects on reduced CrO_x/SiO_2 sites, such as blocking of empty ligand sites (47) or prevention of the reduction of Cr^{3+} to Cr^{2+} (14, 41), and it is clear that the effects cannot easily be assigned.

The observation that H_2 prereduction affected the initial activity led us to believe, however, that the transient behavior of the calcined catalysts was related to the reduction of Cr^{6+} with increasing time on stream. In addition to the possible effects that desorption or rearrangement of entrapped H_2O (or -OH/-H) might have on the initial activity, a careful study of the product distributions, including the release of CO_2, suggested that reduction of the catalyst was not complete after 1 min on stream but continued with longer time on stream. Consideration of the rapid initial decay in the activity of CrS(1.1) from this perspective suggested that it could be due to a reduction of Cr^{3+}, present after 1 min on stream, to 2+ oxidation state. The constant and lower initial activity of H_2-prereduced CrS(1.1) during the first minutes on stream could then be due to a formation of Cr^{2+}/SiO_2 already during the prereduction stage, which would further imply that the reactivity of Cr^{2+}/SiO_2 was lower than that of redox Cr^{3+}/SiO_2.

Contrary to CrS(1.1), the activities of CrS(11) and bulk α-Cr_2O_3 increased between 1 and 3 min on stream, and both catalysts were more active after H_2 prereduction than after calcination (see Figs. 4 and 5). According to H_2-TPR, the reduction of Cr^{6+} on CrS(11) led to the formation of $Cr^{2+}/Cr_2O_3/SiO_2$ and Cr^{3+}/SiO_2, and to Cr^{2+}/Cr_2O_3 in bulk α-Cr_2O_3. From this we conclude that the activation of the catalysts could have been due to a relatively slow reduction of $Cr^{3+}/Cr_2O_3/SiO_2$ to $Cr^{2+}/Cr_2O_3/SiO_2$ with increasing time on stream. This being the case, the reactivity of $Cr^{2+}/Cr_2O_3/SiO_2$ must be considerably higher than that of $Cr^{3+}/Cr_2O_3/SiO_2$ (14). The rapid decay of the activities of CrS(11) and bulk α-Cr_2O_3 would suggest instability of $Cr^{2+}/Cr_2O_3/SiO_2$ under dehydrogenation conditions, however.

In summary, we suggest that on fully reduced CrS(1.1) and CrS(11) (the reduction of which occurred either during H_2 prereduction or with time on *i*-butane stream at 540°C), Cr^{2+}/SiO_2 and $Cr^{2+}/Cr_2O_3/SiO_2$, respectively, serve as active sites in dehydrogenation. In addition, exposed nonredox Cr^{3+} sites, present on both CrS(1.1) and CrS(11), may be active. The uncertainty about the fraction of surface atoms and the presence of coordinatively unsaturated sites complicated the study of the dehydrogenation activity in the nonredox Cr^{3+} phase (1, 35, 37, 46, 48), however. It is worth noting that exposed nonredox Cr^{3+} has been proposed to be active in CrO_x/Al_2O_3 (9, 11), and therefore its activity in CrO_x/SiO_2 could not be ruled out.

So far, the activity of redox Cr^{3+}, present in addition to Cr^{2+}/SiO_2 and $Cr^{2+}/Cr_2O_3/SiO_2$, on fully reduced CrS(3.4), CrS(8.7), and CrS(11), has not been considered in our discussion (see Fig. 6). On the basis of the average dehydrogenation activity (1–10 min on stream), and the concentration of the redox sites on CrO_x/SiO_2 at different Cr loadings, it is proposed that also redox Cr^{3+}/SiO_2 is active in dehydrogenation. This is because the average dehydrogenation activity and the concentration of redox Cr^{3+}/SiO_2 sites increased together with the Cr loading. The proposal that redox Cr^{3+}/SiO_2 sites are active is also in accordance with the findings for CrO_x/Al_2O_3. In the absence of Cr^{2+} sites at low loadings of Cr, the dehydrogenation activity of CrO_x/Al_2O_3 was attributed solely to redox Cr^{3+} (9, 11).

In view of our discussion of the active sites on CrO_x/SiO_2 it would seem that dehydrogenation occurs at diverse sites on the reduced surface, including Cr^{2+}. Accordingly, no specific dehydrogenation site could be distinguished. The way the selectivity of the catalysts varied with Cr loading deserves further comment, however. Namely, both the conversion of *i*-butane and the selectivity to butenes increased with Cr loading (see Table 3). In the presence of equally selective sites at all loadings, the opposite would have been expected, i.e., the selectivity would have been expected to decrease with increasing Cr loading and activity because of the increasing rate of cracking and coke formation with increasing partial pressure of butenes. The increase in the selectivity to butenes with increasing Cr loading led us to conclude that Cr^{2+}/SiO_2 sites were less selective in dehydrogenation than other active sites.

CONCLUSIONS

The structure of CrO_x/SiO_2 catalysts and their activity in the dehydrogenation of *i*-butane were studied. After calcination, 0.8–1.0 wt% Cr was oxidized to 6+ oxidation state, but even at low loadings of Cr, a considerable amount of nonredox Cr^{3+} and α-Cr_2O_3 were formed. According to H_2-TPR measurements, Cr^{6+} existed anchored both to SiO_2 and to α-Cr_2O_3/SiO_2. The dehydrogenation activity of CrO_x/SiO_2 was attributed to redox Cr in 3+ or 2+ oxidation state formed in the reduction of Cr^{6+}. Probably, part of the nonredox Cr^{3+} was also active in dehydrogenation. The relatively low selectivity, i.e., pronounced cracking and coke formation at low loadings of Cr, was attributed to Cr^{2+} directly anchored to SiO_2.

ACKNOWLEDGMENTS

The authors thank Neste Ltd. for cooperation and Academy of Finland for financial support. Ms. Mirja Rissanen, Ms. Päivi Jokimies, and Mr. Asko Sneck are thanked for their contribution in the characterization of the catalysts and Dr. Arla Kytökivi for many helpful discussions.

REFERENCES

1. Poole, C. P., and MacIver, D. S., *Adv. Catal.* **17**, 223 (1967) and references therein.
2. Masson, J., Bonnier, J. M., Duvigneaud, P. H., and Delmon, B., *J. Chem. Soc. Faraday Trans.* **73**, 1471 (1977).
3. Gorriz, O. F., Arrua, L. A., Cadus, L. E., and Rivarola, J. B. P., *Lat. Amer. Appl. Res.* **19**, 31 (1989).
4. DeRossi, S., Ferraris, G., Fremiotti, S., Indovina, V., and Cimino, A., *Appl. Catal.* **106**, 125 (1993).
5. DeRossi, S., Ferraris, G., Fremiotti, S., Garrone, E., Ghiotti, G., Campa, M. C., and Indovina, V., *J. Catal.* **148**, 36 (1994).
6. DeRossi, S., Casaletto, M. P., Ferraris, G., Cimino, A., and Minelli, G., *Appl. Catal.* **167**, 257 (1998).
7. Hakuli, A., Kytökivi, A., Krause, A. O. I., and Suntola, T., *J. Catal.* **161**, 393 (1996).
8. Kytökivi, A., Jacobs, J.-P., Hakuli, A., Meriläinen, J., and Brongersma, H. H., *J. Catal.* **162**, 190 (1996).
9. Cavani, F., Koutyrev, M., Trifirò, F., Bartolini, A., Ghisletti, D., Iezzi, R., Santucci, A., and Del Piero, G., *J. Catal.* **158**, 236 (1996).
10. Weckhuysen, B. M., and Wachs, I. E., *J. Phys. Chem.* **100**, 14437 (1996).
11. Hakuli, A., Kytökivi, A., and Krause, A. O. I., submitted for publication.
12. Weckhuysen, B. M., Verberckmoes, A. A., Buttiens, A. L., and Schoonheydt, R. A., *J. Phys. Chem.* **98**, 579 (1994).
13. Marcilly, Ch., and Delmon, B., *J. Catal.* **24**, 336 (1972).
14. Ashwamy, F., *J. Chem. Soc. Faraday I* **76**, 2096 (1980).
15. Sterligov, O. D., Gitis, K. M., Slovetskaya, K. I., Shpiro, E. S., Rubinshtein, A. M., and Minachev, K. M., *in* "Catalyst Deactivation" (B. Delmon and G. F. Froment, Eds.), Proceedings, 2nd Int. Symp. Catal. Deact., p. 363. Elsevier, Amsterdam, 1980.
16. Lugo, H. J., and Lunsford, J. H., *J. Catal.* **91**, 155 (1985).
17. Slovetskaya, K. I., Sterligov, O. D., and Rubinshtein, A. M., *Neftekhimiya* **35**, 327 (1995).
18. McDaniel, M. P., *Adv. Catal.* **33**, 47 (1985).
19. Wechuysen, B. M., Wachs, I. E., and Schoonheydt, R. A., *Chem. Rev.* **96**, 3327 (1996).
20. Weckhuysen, P. M., Wachs, I. E., and Schoonheydt, R. A., *in* "Preparation of Catalysts VI" (G. Poncelet, Ed.), p. 151. Elsevier, Amsterdam, 1995.
21. Weckhuysen, B. M., De Ridder, L. M., Grobet, P. J., and Schoonheydt, R. A., *J. Phys. Chem.* **99**, 320 (1995).
22. Haukka, S., Lakomaa, E.-L., and Root, A., *J. Phys. Chem.* **97**, 5085 (1993).
23. Haukka, S., *Analyst* **116**, 1055 (1991).
24. Derouane, E. G., Hubin, R., and Mathieu, G., *Chem. Phys. Lett.* **33**, 571 (1975).
25. Jagannathan, K., Srinivasan, A., and Rao, C. N. R., *J. Catal.* **69**, 418 (1981).
26. Zecchina A., Garrone, E., Ghiotti, E., Morterra, C., and Borello, E., *J. Phys. Chem.* **79**, 466 (1975).
27. Rahman, R., Mohamed, M. H., Ahmed, M., and Aitani, A. M., *Appl. Catal.* **12**, 203 (1995).
28. Zaki, M. I., Hasan, M. A., and Fouad, N. E., *Appl. Catal.* **171**, 315 (1998).
29. Curry-Hyde, H. E., Musch, H., and Baiker, A., *Appl. Catal.* **65**, 211 (1990).
30. Hakuli, A., Kytökivi, A., Lakomaa, E.-L., and Krause, A. O. I., *Anal. Chem.* **67**, 1881 (1995).
31. Morrow, B. A., *Stud. Surf. Sci. Catal. A* **57**, 161 (1990).
32. Vansant, E. F., Van Der Voort, P., and Vrancken, K. C., *Stud. Surf. Sci. Catal.* **93**, 357 (1995).
33. Ellison, A., Diakum, G., and Worthington, P., *J. Mol. Catal.* **46**, 131 (1988).
34. Fouad, N. E., Knözinger, H., and Zaki, M. I., *Zeit. Phys. Chem.* **186**, 231 (1994).
35. Ghiotti, G., Garrone, E., Della Gatta, G., Fubini, B., and Giamello, E., *J. Catal.* **80**, 249 (1983).
36. Zecchina, A., Coluccia, S., Cerruti, L., and Borello, E., *J. Phys. Chem.* **75**, 2783 (1971).
37. Burwell, R. L., Haller, G. L., Taylor, K. C., and Read, J. F., *Adv. Catal.* **20**, 1 (1969).
38. McDaniel, M. P., *J. Catal.* **76**, 37 (1982).
39. Ellison, A., NATO Asi, Ser. C, p. 407, 1990.
40. Ellison, A., Overton, T., and Bencze, L., *J. Chem. Soc. Faraday Trans.* **89**, 843 (1993).
41. Groeneveld, C., Wittgen, P. P. M. M., van Kersbergen, A. M., Mestrom, P. L. M., Nuijten, C. E., and Schuit, G. C. A., *J. Catal.* **59**, 153 (1979).
42. Zaki, M. I., Fouad, N. E., Bond, G. C., and Tahir, S. F., *Thermochim. Acta* **285**, 167 (1996).
43. Zaki, M. I., and Knözinger, H., *J. Catal.* **119**, 311 (1989).
44. Hadjiivanov, K., and Busca, G., *Langmuir* **10**, 4534 (1994).
45. Ilieva, L. I., and Andreeva, D. H., *Thermochim. Acta* **265**, 223 (1995).
46. Zecchina, A., Garrone, E., Ghiotti, G., Morterra, C., and Borello, E., *J. Phys. Chem.* **79**, 966 (1975).
47. Wittgen, P. P. M. M., Groeneveld, C., Zwaans, P. J. C. J. M., Morgenstern, H. J. B., van Heughten, A. H., van Heumen, C. J. M., and Schuit, G. C.A., *J. Catal.* **77**, 360 (1982).
48. Zecchina, A., Coluccia, S., Guglielminotti, E., and Ghiotti, G., *J. Phys. Chem.* **75**, 2774 (1971).